Development/Plasticity/Repair

Atypical Protein Kinase C Regulates Primary Dendrite Specification of Cerebellar Purkinje Cells by Localizing Golgi Apparatus

Koji Tanabe,[1] Shuichi Kani,[1,2] Takashi Shimizu,[1,3] Young-Ki Bae,[1,4] Takaya Abe,[2] and Masahiko Hibi[1,3]

[1]Laboratory for Vertebrate Axis Formation, and [2]Laboratory for Animal Resources and Genetic Engineering, RIKEN Center for Developmental Biology, Kobe, Hyogo 650-0047, Japan, [3]Bioscience and Biotechnology Center, Nagoya University, Nagoya, Aichi 464-8601, Japan, and [4]Division of Basic and Applied Sciences, Research Institute, National Cancer Center, Goyang 410-769, Republic of Korea

Neurons have highly polarized structures that determine what parts of the soma elaborate the axon and dendrites. However, little is known about the mechanisms that establish neuronal polarity *in vivo*. Cerebellar Purkinje cells extend a single primary dendrite from the soma that ramifies into a highly branched dendritic arbor. We used the zebrafish cerebellum to investigate the mechanisms by which Purkinje cells acquire these characteristics. To examine dendritic morphogenesis in individual Purkinje cells, we marked the cell membrane using a Purkinje cell-specific promoter to drive membrane-targeted fluorescent proteins. We found that zebrafish Purkinje cells initially extend multiple neurites from the soma and subsequently retract all but one, which becomes the primary dendrite. In addition, the Golgi apparatus specifically locates to the root of the primary dendrite, and its localization is already established in immature Purkinje cells that have multiple neurites. Inhibiting secretory trafficking through the Golgi apparatus reduces dendritic growth, suggesting that the Golgi apparatus is involved in the dendritic morphogenesis. We also demonstrated that in a mutant of an atypical protein kinase C (aPKC), Prkci, Purkinje cells retain multiple primary dendrites and show disrupted localization of the Golgi apparatus. Furthermore, a mosaic inhibition of Prkci in Purkinje cells recapitulates the aPKC mutant phenotype. These results suggest that the aPKC cell autonomously controls the Golgi localization and thereby regulates the specification of the primary dendrite of Purkinje cells.

Introduction

Each type of neuron has a specific pattern of dendrites. Since dendritic morphology directly determines neuronal inputs, it must be tightly regulated. Dendritic patterning can be divided into three stages: extension of primary dendrite(s) from the soma, growth of dendritic arbors, and branching. Although a number of transcriptional, intracellular signaling, and extracellular molecules are known to regulate dendritic growth or branching (Parrish et al., 2007; Jan and Jan, 2010), how the number of primary dendrites is controlled is unknown.

Although cerebellar Purkinje cells have extensively branched dendritic trees, they have a single primary dendrite, which makes them a good model for studying dendritic patterning. The development of Purkinje cell dendrites has been well characterized in rodents (Armengol and Sotelo, 1991; Kapfhammer, 2004). Initially, Purkinje cells extend many short processes and have a brushy morphology, termed "stellate with disoriented dendrites." Following this phase, asymmetric dendritic morphology is established by the extension of a single permanent dendrite and the retraction of the other processes. The Purkinje cells keep only the one primary dendrite as they acquire their mature polarized morphology (Armengol and Sotelo, 1991; Kapfhammer, 2004).

There have been many *in vitro* studies of neuronal polarization focusing on axon specification. For example, cultured hippocampal neurons initially form lamellipodia, which subsequently become fine neurites (Dotti et al., 1988). With time, one of the neurites becomes a morphologically identifiable axon, and the others become dendrites. Complex networks of molecules that regulate axon specification have been reported (Arimura and Kaibuchi, 2007), and key proteins include Par3, Par6, and atypical protein kinase C (aPKC), which constitute the Par complex. These proteins localize to the nascent axon in cultured neurons, and their inhibition or overexpression disrupts axon specification (Shi et al., 2003). However, some *in vivo* experiments do not support an important role for the Par complex in axon specification (Rolls and Doe, 2004; Zolessi et al., 2006). Thus, the role played by the Par complex, including aPKC, in neuronal polarization is still controversial.

Here, we used zebrafish to study dendritic morphogenesis of Purkinje cells. As in mammals (Hoshino et al., 2005), zebrafish Purkinje cells are derived from neuronal progenitors that have a simple epithelial morphology and are located in the ventricular zone of the anterior hindbrain (Bae et al., 2009; Kani et al., 2010).

Received June 29, 2010; revised Sept. 29, 2010; accepted Oct. 15, 2010.

K.T. was a recipient of the Special Postdoctoral Researcher program of RIKEN. This work was supported by grants from RIKEN and The Uehara Memorial Foundation (to M.H.). We thank J. Malicki for the *prkci* mutant; H. Okamoto for the *HuC:Kaede* plasmid; A. M. Reugels for the Pard3-EGFP plasmid; D. Stainier for the EGFP-Pard6 plasmids; K. Bando, S. Fujii, and A. Katsuyama for technical assistance; and the members of the Hibi Laboratory for helpful discussions.

Correspondence should be addressed to Masahiko Hibi, Bioscience and Biotechnology Center, Nagoya University, Furocho, Chikusaku, Nagoya 464-8601, Japan. E-mail: hibi@bio.nagoya-u.ac.jp.

K. Tanabe's present address: Division of Stem Cell Regulation Research, Osaka University Graduate School of Medicine, Osaka 565-0871, Japan.

DOI:10.1523/JNEUROSCI.3352-10.2010

 0270-6474/10/3016983-10$15.00/0

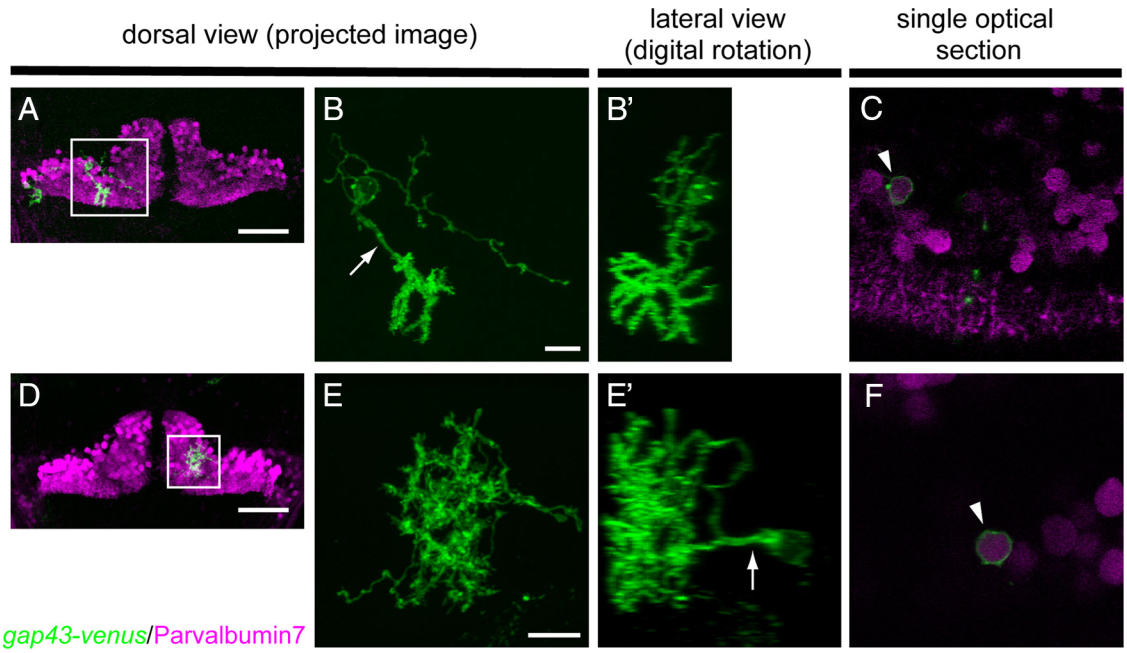

Figure 1. Dendritic morphology of zebrafish Purkinje cells. ***A***, ***D***, Dorsal view images of the cerebellum of 8 dpf larvae that were injected with *aldoca:gap43-Venus* plasmid and mosaically expressed gap43-Venus in the Purkinje cells. Two Purkinje cells in ***A*** and one in ***D*** expressed gap43-Venus (green). All the Purkinje cells were labeled with an anti-parvalbumin7 antibody (magenta). Purkinje cells surrounded by boxes were subjected to observation at a higher resolution (***B***, ***B′***, ***C***, ***E***, ***E′***, ***F***). Scale bars, 20 μm. ***B***, ***B′***, Dendritic morphology of a relatively posterolateral Purkinje cell labeled with gap43-Venus, boxed in ***A***. ***B***, Projected image of serial confocal optical sections taken from the dorsal side. The Purkinje cell extended a single primary dendrite (arrow) posteriorly. Dense dendritic spines were observed at the dendritic terminals. ***B′***, Lateral view constructed digitally. Dendritic arbors expanded along the dorsoventral axis. Scale bar, 10 μm. ***E***, ***E′***, Dendritic morphology of an anteromedial Purkinje cell, boxed in ***D***. ***E***, Dorsal view with a projected image. ***E′***, Lateral view. The Purkinje cell extended a single primary dendrite dorsally, and the dendritic arbors were randomly distributed. ***C***, ***F***, Single optical sections at the level of the soma of the posterolateral (***C***) and anteromedial (***F***) Purkinje cells shown in ***B*** and ***E***, respectively. The gap43-Venus-expressing Purkinje cells were positive for parvalbumin7 (magenta). Scale bar, 10 μm.

The progenitors migrate dorsally to differentiate into Purkinje cells, which have complex dendritic arbors. However, the molecular details of Purkinje cell morphogenesis remain to be elucidated.

Although Purkinje cells *in vitro* develop multiple dendrites, they do not refine the dendrites to a single primary one (Hirai and Launey, 2000; Tanaka et al., 2006). Therefore, *in vivo* analyses are required to understand the mechanism of primary dendrite specification. Here, we examined this mechanism by marking the cell membrane and Golgi apparatus with fluorescent proteins expressed under a Purkinje cell-specific promoter. Our data provide *in vivo* evidence that aPKC regulates the primary dendrite specification of Purkinje cells by regulating the location of the Golgi apparatus. This is a previously unrecognized mechanism for controlling the number of primary dendrites.

Materials and Methods

Zebrafish wild-type, mutant and transgenic lines, maintenance, staging, and chemical treatment. Wild-type zebrafish (*Danio rerio*) with the Oregon AB genetic background were used. The *heart and soul* (*has*; *prkci*^{m567}) mutant was previously described (Horne-Badovinac et al., 2001). Zebrafish were reared as described in (Westerfield, 1993). For all the imaging experiments, at 12 h postfertilization (hpf) 1-phenyl-2-thiourea (PTU) was added to the embryo medium to a final concentration of 0.005% (w/v) to block the development of pigmentation. Developmental stages were determined as previously described (Kimmel et al., 1995). To inhibit the Golgi apparatus-mediated transport, Brefeldin A (BFA) (Sigma) was added to the embryo medium at a concentration of 1 μg/ml.

DNA constructs. To isolate the *aldoca* (aldolase c, fructose-biphosphate, a; Zebrafish Information Network: http://zfin.org) promoter, we obtained bacterial artificial chromosome DKEY-145M5, which contains a ~49 kbp genomic fragment, 5′ upstream of the translation initiation site of the *aldoca* gene. We excised the ~5 kbp fragment that contains promoter region, first exon, first intron, and a short fragment of the second exon of *aldoca* by PCR with the primers 5′-ACGCGAGTTATTCAATGAGCCCCT-3′ and 5′-GGACAGTACAGATGAGGCCCTGTT-3′, and fused it to the *gap43-Venus*-poly A cassette. The *aldoca:gap43-Venus-pA* cassette was then inserted into the pT2K plasmid, which contains Tol2 transposase recognition elements (Kawakami et al., 2004). The membrane-tagged Venus (Nagai et al., 2002) and mCherry (Shaner et al., 2004) cDNAs (*gap43-Venus* and *gap43-mCherry*) were constructed by fusing each of them to a fragment encoding the first 20 aa of the zebrafish *gap43* gene, which contains a palmitoylation site and targets the fusion protein to the cell membrane (Okada et al., 1999; Kay et al., 2004). Golgi-Venus is a fusion protein of the N-terminal 81 aa of mouse UDP-galactose:β-D-*N*-acetylglucosaminide β-1,4-galactosyltransferase and Venus, and it localizes to the Golgi apparatus (Llopis et al., 1998). To express Golgi-Venus and gap43-mCherry simultaneously in the same cell, we linked the two cDNA fragments with one corresponding to the 2A peptide of porcine teschovirus-1 (PTV1), as described previously (Provost et al., 2007). To construct *elavl3:myc-prkci*^{2A}, we replaced the Kaede cassette in the *elavl3:Kaede* (HuC:Kaede) plasmid (Sato et al., 2006) with *his-myc-prkci*^{2A} (Rohr et al., 2006).

Plasmid injection and generation of a transgenic line. For the mosaic gene expression, circular plasmids were injected into fertilized eggs at the one-cell stage, according to standard procedures (Stuart et al., 1988; Higashijima et al., 1997). Approximately 10 pg of the plasmid was injected into each egg. The *Tg(aldoca:gap43-Venus)* transgenic lines were generated by using the Tol2 transposon method (Kawakami et al., 2004).

Live confocal imaging. Before imaging, the chorion was manually removed and the larva transferred to a solution of embryo medium containing 0.005% PTU and 0.02% (w/v) tricaine. Each larva was then embedded in 0.7% low-melting-point agarose and dissolved in embryo medium containing PTU and tricaine in a glass-bottomed dish. Confocal images were obtained using either a Carl Zeiss LSM510 or LSM-PASCAL microscope equipped with a 63×/1.2 numerical aperture (NA) water-immersion or 40×/1.3 NA oil-immersion objective. To reconstruct the confocal stacks, a series of optical sections was collected in the *z* dimen-

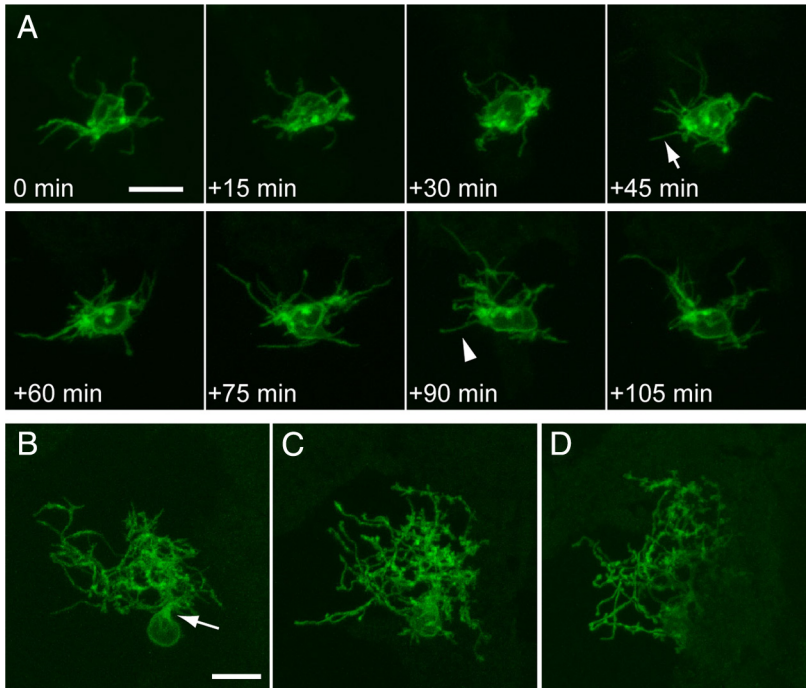

Figure 2. Purkinje cells initially extend multiple neurites and become morphologically mature by retracting these transient neurites. ***A***, Dynamic morphological remodeling of Purkinje cells ~3 dpf. A medially located Purkinje cell expressing gap43-Venus was subjected to time-lapse confocal imaging. The imaging started at 76 hpf (0 min), and images were taken at 15 min intervals. The neurite indicated by an arrow was newly formed within 15 min, and the one indicated by an arrowhead was retracted within 15 min. ***B–D***, Morphology of the Purkinje cell shown in ***A*** at 4, 5, and 6 dpf, respectively. The Purkinje cell completed its primary dendrite specification and extended a single primary dendrite by 4 dpf (***B***, arrow). After 4 dpf, further dendritic branching took place, and dendritic spines formed. Scale bars: ***C***, ***D***, 10 μm. ***B–D*** are shown in the same scale.

sion (*z*-stack) and projected as a single image or reconstructed in three dimensions to provide views of the image stack at different angles. The step size for each *z*-stack was chosen upon calculation of the theoretical *z*-resolution of the objective used (typically 0.5–1.0 μm). Time-lapse imaging was performed by collecting the *z*-stacks encompassing the same cells at 15 min intervals.

Immunohistochemistry and statistical analysis. For immunostaining, anti-parvalbumin7 (1:1000 dilution, mouse ascites) (Bae et al., 2009), anti-green fluorescent protein (GFP) (1:1000 dilution, rat ascites, Nacalai), anti-DsRed (1:1000 dilution, rabbit polyclonal, Clontech), anti-GM130 (1:200 dilution, mouse monoclonal, BD Transduction Laboratories), and anti-c-myc (1:500 dilution, mouse monoclonal, Santa Cruz Biotechnology) antibodies were used. For whole-mount immunostaining, zebrafish larvae were fixed at room temperature in 4% paraformaldehyde in PBST (PBS, 0.1% Triton X-100) for 2 h. The samples were then incubated in 5% goat serum (Vector Laboratories), PBS-DT (PBS, 1% BSA, 1% DMSO, 1% Triton X-100) at room temperature for 1 h for blocking, and reacted with the primary antibody diluted in PBS-DT at 4°C overnight. After six washes with PBST, the samples were incubated with secondary antibodies (1:1000 dilution, Alexa Fluor 488 goat-anti-rat, Alexa Fluor 555 or 647 goat anti-mouse, and Alexa 555 goat anti-rabbit IgG heavy and light chains, Invitrogen). After six washes with PBST, the samples were embedded in 0.7% low-melting-point agarose dissolved in PBS in a glass-bottomed dish, and subjected to confocal imaging, as described above. The Golgi localization index was calculated as the percentage of the area of the Golgi-Venus signal over the area of the soma visualized with gap43-mCherry. To measure the area of the dendritic fields, the Golgi area, and the somal area, we converted the projected images to binary data, and the total number of pixels was counted using ImageJ software (National Institutes of Health). Each area was then calculated from the number of pixels. The image-capturing conditions, such as detector gains, pinholes, laser output, and the threshold for the binary data, were kept constant. For statistical analysis, the two-tailed Welch *t* test was used.

Results

Dendritic morphology of Purkinje cells in the zebrafish cerebellum

To mark Purkinje cells by expressing a transgenic fluorescent protein, we sought a zebrafish Purkinje cell-specific promoter. After testing the upstream sequences of several genes that are expressed in Purkinje cells, we identified the promoter of the *aldoca* gene as a driver for Purkinje cell-specific gene expression. Aldolase C is the antigen of the zebrin II antibody, which marks a subset of Purkinje cells in the rodent and avian cerebellum (Lannoo et al., 1991b; Ozol et al., 1999; Marzban et al., 2010) and all the Purkinje cells in the cerebellum of teleosts, including zebrafish (Brochu et al., 1990; Lannoo et al., 1991a,b; Meek et al., 1992; Bae et al., 2009). Zebrafish has two copies of the *aldolase c* gene, and only one of them, *aldoca* (also known as *aldocl*), is expressed in Purkinje cells (Bae et al., 2009).

We detected *aldoca* mRNA expression at ~72 hpf. We isolated an ~5 kb fragment extending upstream from the translational initiation site of the *aldoca* gene and fused it to a cDNA encoding membrane-targeted Venus fluorescent protein (gap43-Venus). We confirmed that the gap43-Venus expression in Purkinje cells was specific by injecting the *aldoca:gap43-Venus* plasmid DNA and established a stable transgenic line *Tg(aldoca:gap43-Venus)* by using the Tol2 transposon-mediated transgene method (Kawakami et al., 2004). In the transgenic larvae, gap43-Venus expression was detected in Purkinje cells from ~72 hpf, consistent with the onset of endogenous *aldoca* mRNA expression. The gap43-Venus transgene was exclusively expressed in Purkinje cells, which was confirmed by colocalization with the Purkinje cell marker parvalbumin7 (Bae et al., 2009) (supplemental Fig. 1, available at www.jneurosci.org as supplemental material).

To observe the Purkinje cells' morphology at single-cell resolution, we injected the *aldoca:gap43-Venus* plasmid into one-cell-stage embryos. Since plasmid injection into early-stage zebrafish embryos results in the mosaic expression of transgenes, we obtained mosaic labeling of the Purkinje cells. Approximately 5% of the injected larvae showed a mosaic expression of gap43-Venus in their Purkinje cells at 8 d postfertilization (dpf) (Fig. 1*A*,*D*). By observing the fluorescent dendrites, we found that the Purkinje cells displayed diverse dendritic morphologies. The Purkinje cells located in the posterolateral cerebellum extended a single primary dendrite to the posterior side, and their distal dendritic arbors extended along the dorsoventral and anteroposterior plane forming a relatively planar pattern (Fig. 1*B*,*B*′). In contrast, Purkinje cells located in the anteromedial domain extended the primary dendrite dorsally, and their extensively branched dendritic arbors did not exhibit a planar pattern (Fig. 1*E*,*E*′). All the gap43-Venus-expressing cells were positive for parvalbumin7 ($n = 30$) (Fig. 1*C*,*F*), confirming that they were differentiated Purkinje cells. Despite the morphological diversity, all the Purkinje cells had a single primary dendrite, as observed in the mammalian cerebellum.

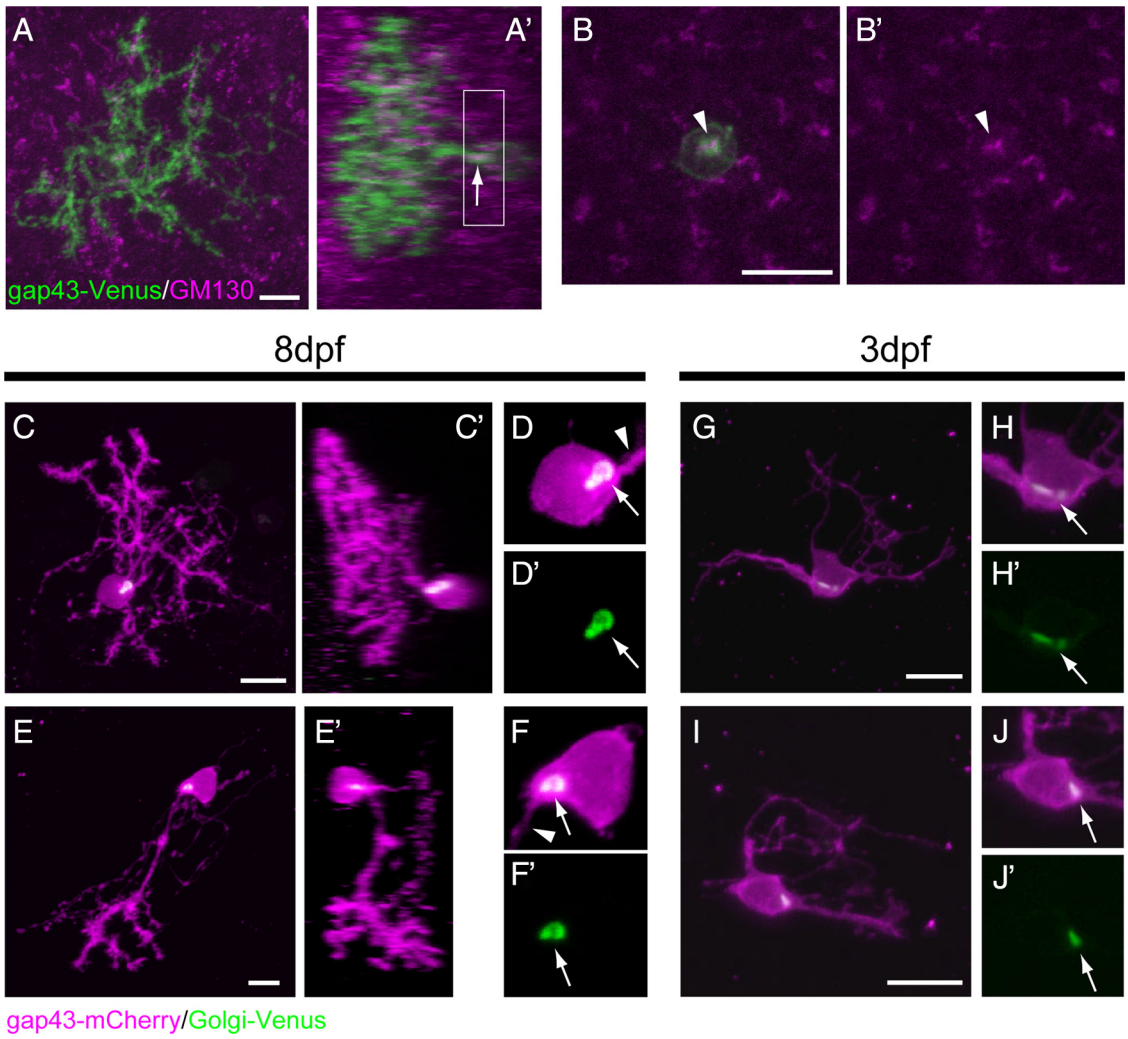

Figure 3. Golgi apparatus is exclusively localized to the root of the primary dendrite, and this localization precedes the primary dendrite specification. ***A–B′***, A Purkinje cell expressing gap43-Venus (green) in an 8 dpf larva that was immunostained with the GM130 antibody (magenta). ***A***, ***A′***, A dorsal view projected image (***A***) and a lateral view constructed digitally (***A′***). The GM130-positive Golgi was localized to the root of the primary dendrite (small arrow). ***B***, ***B′***, Higher-magnification views of the projected image of optical sections corresponding to the boxed area in ***A′***. The GM130 signal was only observed at the root of the primary dendrite (arrowheads). ***C–J′***, Purkinje cells in larvae expressing the *aldoca:gap43-mCherry-PTV1–2A-Golgi-Venus* plasmid. Using the 2A peptide system, the cellular morphology was visualized with gap43-mCherry (magenta), and the Golgi apparatus was visualized with Golgi-Venus (green). ***C–E′***, Purkinje cells in 8 dpf larvae. Dorsal (***C***, ***E***, projected images) and lateral (***C′***, ***E′***, constructed digitally) views of anteromedial (***C***, ***C′***) and posterolateral (***E***, ***E′***) Purkinje cells. ***D***, ***D′***, and ***F***, ***F′*** are high-magnification views of a single optical section of the Purkinje cells in ***C*** and ***E***, respectively. The Golgi apparatuses that were visualized with Golgi-Venus (arrows) were exclusively localized to the root of the primary dendrites (arrowheads). ***G***, ***I***, Dorsal view projected images of Purkinje cells in 3 dpf larvae. ***H***, ***H′*** and ***J***, ***J′*** are high-magnification views of a single optical section in the Purkinje cells in ***G*** and ***I***, respectively. At this stage, Purkinje cells had multiple primary dendrites and did not exhibit morphological polarity, but the Golgi apparatus was already localized to a restricted area (arrows). Scale bars, 10 μm.

Rapid remodeling of Purkinje cells' morphology ~3 dpf

Next, we performed a developmental observation of the morphological changes of Purkinje cells in zebrafish. Purkinje cells initially extend multiple neurites that form a "disoriented shape" in the mammalian cerebellum at early postnatal stages (Kapfhammer, 2004). Similarly, at 3 dpf, when the gap43-Venus expression started, Purkinje cells had multiple neurites and did not show any morphological polarity in their elongation (Fig. 2*A*). Time-lapse observation revealed that the Purkinje cells rapidly remodeled their morphology by extending and retracting neurites at this "multipolar" phase (Fig. 2*A*). In a typical case, a neurite was formed (Fig. 2*A*, arrow) or retracted within 15 min (Fig. 2*A*, arrowhead). By 4 dpf, the Purkinje cells had retracted all but a single primary dendrite and an axon (Fig. 2*B*). After 4 dpf, we observed further branching of the terminal dendritic arbors and the extensive formation of dendritic spines (Fig. 2*C*,*D*). These data show that Purkinje cells select a single primary dendrite from among multiple transient ones.

Golgi apparatus is exclusively localized to the root of the primary dendrite

We next investigated the mechanisms that specify a single primary dendrite of Purkinje cells. It is reported that the Golgi apparatus is preferentially localized to the proximal portion of apical dendrites in rodent hippocampal and cortical pyramidal neurons, and that directed post-Golgi trafficking plays a role in asymmetric dendrite growth (Horton et al., 2005). This led us to hypothesize that the Golgi apparatus is located preferentially at the single primary dendrite of Purkinje cells. We immunostained 8 dpf larvae expressing the *aldoca:gap43-Venus* plasmid with a *cis*-Golgi marker, GM130 (Fig. 3*A–B′*). The gap43-Venus-rich structures that were colabeled with the GM130 antibody were

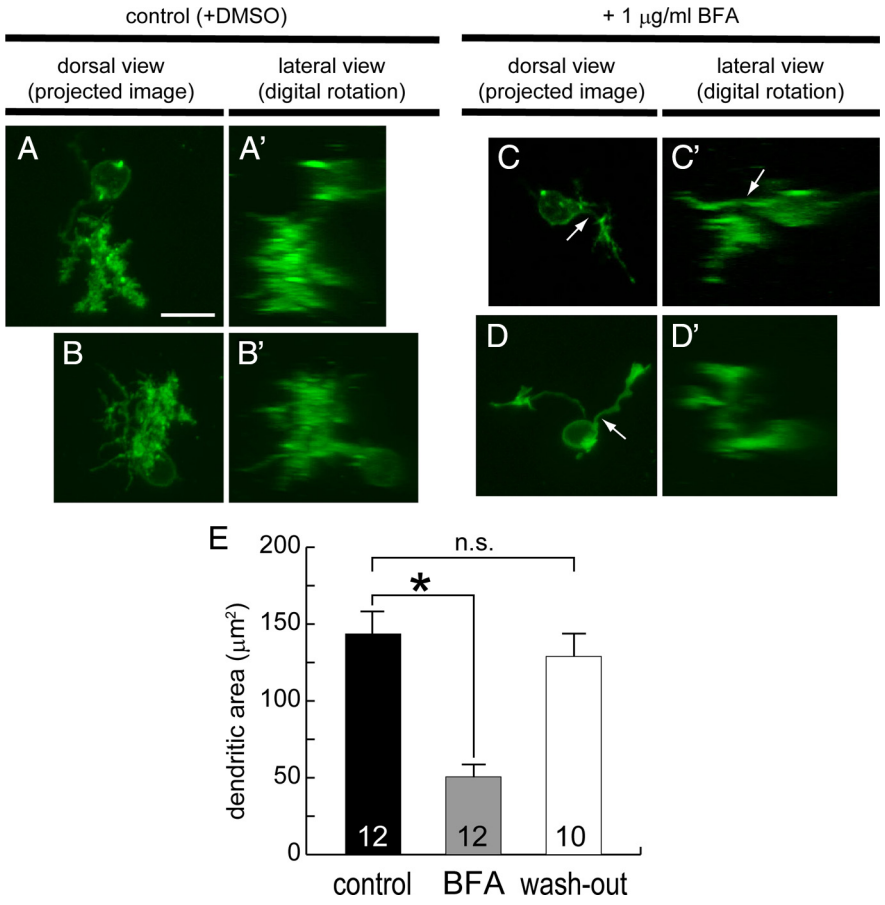

Figure 4. Dendritic growth is suppressed by BFA treatment. ***A–D′***, Purkinje cells expressing gap43-Venus in 5 dpf larvae were treated with DMSO (as control) (***A–B′***) or 1 μg/ml BFA (***C–D′***) from 2.5 to 5 dpf. ***A–D***, Dorsal view projected images. ***A′–D′***, Digitally synthesized lateral view images of ***A–D***, respectively. ***A–B′***, A posterolateral Purkinje cell (***A***, ***A′***) and an anteromedial Purkinje cell (***B***, ***B′***). Although extensive branching and dense dendritic spines were observed in control Purkinje cells (***A***, ***B***), the Purkinje cells in BFA-treated larvae had a single primary dendrite (arrows) but exhibited a simple dendritic morphology (***C***, ***D***). ***E***, Graph of the dendritic area of Purkinje cells in control and BFA-treated larvae. Larvae were treated with DMSO (control, black bar), or 1 μg/ml BFA from 2.5 to 5 dpf (gray bar) or from 2.5 to 4 dpf (BFA was washed out at 4 dpf, white bar). Dendritic area was determined at 5 dpf. Dendritic area was significantly reduced in the Purkinje cells of the larvae treated with BFA from 2.5 to 5 dpf (*$p < 0.001$ by Welch's *t* test). Purkinje cells in the larvae that were treated from 2.5 to 4 dpf had a similar size of dendritic area, compared with control Purkinje cells ($p > 0.1$). Error bars show SEM numbers inside the bars represent the number of cells tested. All images were taken at the same scale. Scale bar, 10 μm.

located at the root of the primary dendrite of the Purkinje cells (Figs. 3*A′*, arrow, 3*B*,*B′*, arrowheads), indicating that the Golgi apparatus was positioned at the root of the primary dendrite.

To obtain a clearer image of the Golgi, we simultaneously expressed membrane-targeted red fluorescent protein (gap43-mCherry) and a Golgi apparatus-targeted Venus (Golgi-Venus) (Llopis et al., 1998) by using the viral 2A peptide system (Provost et al., 2007). In this experiment, gap43-mCherry and Golgi-targeted Venus were expressed under the control of the *aldoca* promoter in a small number of Purkinje cells. We found that the Golgi-Venus was exclusively located at the root of the primary dendrite in Purkinje cells in both the anteromedial (Fig. 3*C–D′*) and posterolateral (Fig. 3*E–F′*) domains at 8 dpf. Thus, the Golgi apparatus is exclusively positioned at the root of the primary dendrite in mature Purkinje cells, which suggests a role for Golgi localization in the primary dendrite specification. However, it was also possible that the Golgi's location was the result, not the cause, of this process. To address these possibilities, we performed a simultaneous imaging of dendrite formation and Golgi localization in 3 dpf larvae expressing the *aldoca:gap43-mCherry-PTV1-2A-Golgi-Venus* plasmid. As described above, the Purkinje cells extended multiple neurites in random directions and did not show a morphological preference for the primary dendrite at this stage. However, the Golgi apparatus was restricted to a small part of the soma, located near the root of one of neurites (Fig. 3*G–J′*), which suggested that the Golgi localization precedes the primary dendrite specification. These data imply a role for Golgi localization in the specification of primary dendrites.

Forward secretory trafficking is necessary for the proper dendritic growth of Purkinje cells

To examine whether secretory trafficking through the Golgi apparatus was involved in the dendritic morphogenesis of Purkinje cells, we used BFA, a fungal macrocyclic lactone that inhibits the secretory pathway by disassembling the Golgi apparatus (Klausner et al., 1992). BFA treatment inhibits the dendritic growth of cultured rodent hippocampal and cortical pyramidal neurons (Horton et al., 2005). We treated zebrafish larvae expressing gap43-Venus in Purkinje cells with 1 μg/ml BFA between 2.5 and 5 dpf and examined them at 5 dpf. The Purkinje cells of control larvae at 5 dpf displayed extensively branched dendritic arbors and dense dendritic spines (Fig. 4*A–B′*). In contrast, the Purkinje cells of the BFA-treated larvae had much simpler dendrites, without highly ordered dendritic branches or spines (Fig. 4*C–D′*), although they had a single primary dendrite (12/12) (Fig. 4*C–D′*, arrows). Since the dendritic patterns of the control Purkinje cells were too complex to trace all the branches and measure the dendritic length, we measured their dendritic area by counting the pixels of the gap43-Venus signal in digital images. The dendritic area of the Purkinje cells in control larvae was 143.5 μm^2 on average ($n = 12$, SEM = 14.95 μm^2). In contrast, the Purkinje cells in the BFA-treated larvae showed a much smaller dendritic area (50.59 μm^2 on average, $n = 12$, SEM = 8.382 μm^2, $p < 0.0001$) (Fig. 4*E*). We also performed a "wash-out" experiment, in which we treated zebrafish larvae with 1 μg/ml BFA between 2.5 and 4 dpf, and washed out the BFA to examine the dendritic morphology at 5 dpf. Purkinje cells in these larvae had a similar size of dendritic area compared with Purkinje cells in control larvae (129.0 μm^2 on average, $n = 10$, SEM = 14.77 μm^2, $p > 0.1$) (Fig. 4*E*). These results indicate that the secretory trafficking through the Golgi apparatus is necessary for the dendritic growth of Purkinje cells; Purkinje cells are able to resume the dendritic growth after inhibition of the Golgi-mediated secretory trafficking.

Purkinje cells retain multiple primary dendrites, and the Golgi localization is disrupted in an aPKC mutant

Our findings suggested that the specification of a single primary dendrite in Purkinje cells is regulated by the localized Golgi ap-

paratus. We next investigated the molecular mechanism that controls the Golgi localization. To address this issue, we took a candidate approach. Studies of zebrafish mutants with defective retinal layer development have identified genes involved in cell-polarity determination, like *erythrocyte membrane protein band 4.1 like 5* (*mosaic eyes*) (Jensen and Westerfield, 2004), *crumbs homolog 2* (*oko meduzy*) (Omori and Malicki, 2006), *MAGUK p55 subfamily member 5a* (*nagie oko*) (Wei and Malicki, 2002), and a *protein kinase C ι* (*prkci*, *heart and soul*: *has*) (Horne-Badovinac et al., 2001). We examined the Purkinje cells' morphology in these mutants and found that they retained multiple primary dendrites at 4 dpf in the *prkci* mutant larvae.

Prkci is also called protein kinase λ and is a member of the aPKC family. aPKCs constitute an evolutionarily conserved protein complex, containing Par3, Par6, and Cdc42, that regulates various kinds of cell polarities (Suzuki and Ohno, 2006). Because the *prkci* mutant was lethal at ~5 dpf, we performed the Purkinje cell imaging at 4.5 dpf. Although most, if not all, of the Purkinje cells in the control larvae had completed their primary dendrite specification and extended only a single primary dendrite by this stage ($n = 12$), 58.3% of the *prkci* mutant Purkinje cells still possessed multiple neurites (Fig. 5*B*,*E*, arrowheads) ($n = 12$). Since the apico-basal polarity of neuroepithelial cells is disrupted in the *prkci* mutant (Horne-Badovinac et al., 2001), this finding might have simply reflected the immaturity of the mutant Purkinje cells. However, the mutant Purkinje cells correctly expressed parvalbumin7 (Fig. 5*C*,*F*, arrows) ($n = 12$). In addition, the expression of the *aldoca:gap43-Venus* transgene was normal for this stage. Therefore, the labeled cells had apparently differentiated into mature Purkinje cells; these results reveal that the function of aPKC Prkci is necessary for their primary dendrite specification.

We expected that the "multidendrite" phenotype of the *prkci* mutant larvae was due to the mislocalization of the Golgi apparatus. To find out, we monitored the dendritic morphology and Golgi localization in *prkci* mutant larval Purkinje cells expressing gap43-mCherry and Golgi-Venus. In the Purkinje cells of control larvae at 4.5 dpf, Golgi-Venus was detected exclusively at the root of the primary dendrite (Fig. 6*A–D*). In the *prkci* mutants, strong Golgi-Venus labeling was present in a restricted region of the Purkinje cell somata, but an additional uniform distribution of Golgi-Venus along the plasma membrane was also observed (Fig. 6*E–F′*). In some cases, multiple spots of Golgi-Venus labeling were observed (Fig. 6*G–H′*). We calculated a "Golgi localization index" as the percentage of the area labeled by Golgi-Venus over the somal area (details in Materials and Methods). In the control Purkinje cells, the Golgi localization index was 7.44 on average ($n = 13$, SEM = 0.584). In contrast, the Golgi localization index in the *prkci* mutant Purkinje cells was 13.5 on average ($n = 11$, SEM = 1.79), which is a statistically significant increase ($p < 0.01$). These results indicated that the Golgi apparatus was distributed over a greater area of the Purkinje cells in the *prkci* mutant cerebellum (Fig. 6*I*) than in the controls.

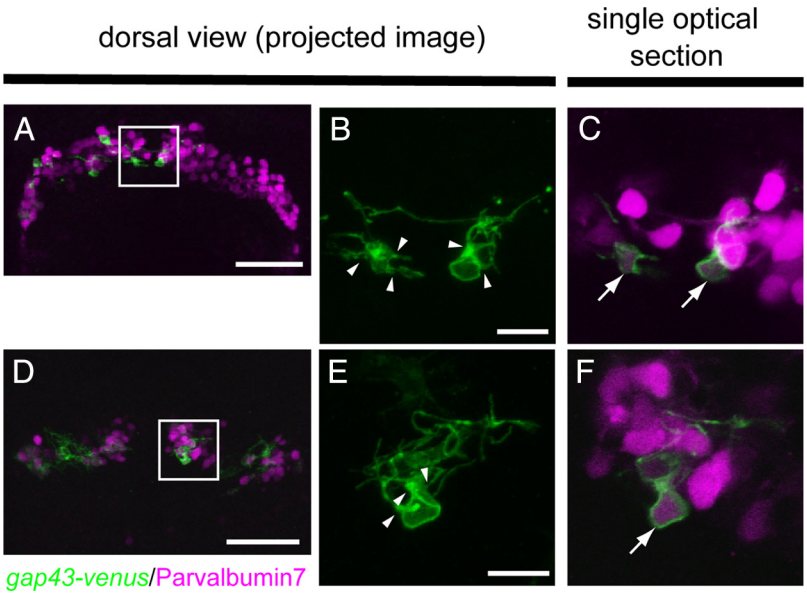

Figure 5. Purkinje cells retain multiple primary dendrites in a *prkci* mutant. ***A***, ***D***, Dorsal views of 4.5 dpf *prkci* mutant larvae expressing *aldoca:gap43-Venus* (green). All the Purkinje cells were stained with an anti-parvalbumin7 antibody (magenta). Scale bars, 50 μm. ***B***, ***C***, ***E***, ***F***, Boxed areas (medial domains) in ***A*** and ***D*** are shown as high-magnification images in ***B*** and ***E***, respectively. ***B***, ***E***, Only the gap43-Venus images are shown. ***C*** and ***F*** are a single optical section of ***B*** and ***E***, respectively, also showing the parvalbumin7 signal. Although the Purkinje cells in the *prkci* mutant expressed parvalbumin7 (arrows in ***C***, ***F***), they retained multiple primary dendrites (***B***, ***E***, arrowheads). Scale bars, 10 μm.

These data suggest that the aPKC Prkci is required for the correct positioning of the Golgi apparatus, and that the multidendrite phenotype of the Purkinje cells in the *prkci* mutant larvae was due to its mislocalization.

aPKC is required cell autonomously for localizing the Golgi and the subsequent primary dendrite specification

Aberrant neuroepithelial architectures are seen in various brain regions of the *prkci* mutants (Horne-Badovinac et al., 2001). Thus, defects in cells other than Purkinje cells might secondarily affect the primary dendrite specification of Purkinje cells. To exclude this possibility, we examined whether Prkci functions cell autonomously in the Golgi's localization and the primary dendrite specification. We mosaically inhibited the function of Prkci by expressing a kinase-inactive form of Prkci (Prkci^{2A}), which functions as a dominant-negative molecule (Rohr et al., 2006), under the control of the pan-neuronal *elav-like 3* (*elavl3*, also called *HuC*) promoter, which drives expression in postmitotic neurons (Park et al., 2000; Higashijima et al., 2003; Sato et al., 2006). We injected *elavl3:myc-prkci^{2A}* and *aldoca:gap43-mCherry-2A-Golgi-Venus* plasmids into one-cell-stage embryos and performed the imaging at 5 dpf, when most Purkinje cells have finished their primary dendrite specification and have only a single primary dendrite.

Whereas all the control Purkinje cells had a single primary dendrite ($n = 12$) (Fig. 7*A–D′*), 41.7% of the *prkci^{2A}*-expressing Purkinje cells, which were labeled with the myc epitope, had multiple primary dendrites ($n = 12$) (Fig. 7*E–H′*). As observed in the *prkci* mutants, disruption of the Golgi localization was observed in all the *prkci^{2A}* -expressing Purkinje cells. We then calculated the Golgi localization index. In the control Purkinje cells, the Golgi localization index was 7.86 ($n = 12$, SEM = 0.819). In the *prkci^{2A}*-expressing Purkinje cells, the Golgi localization index was significantly increased (11.4, $n = 12$, SEM = 0.857; $p < 0.01$) (Fig. 7*I*). These results showed that the mosaic inhibition of the

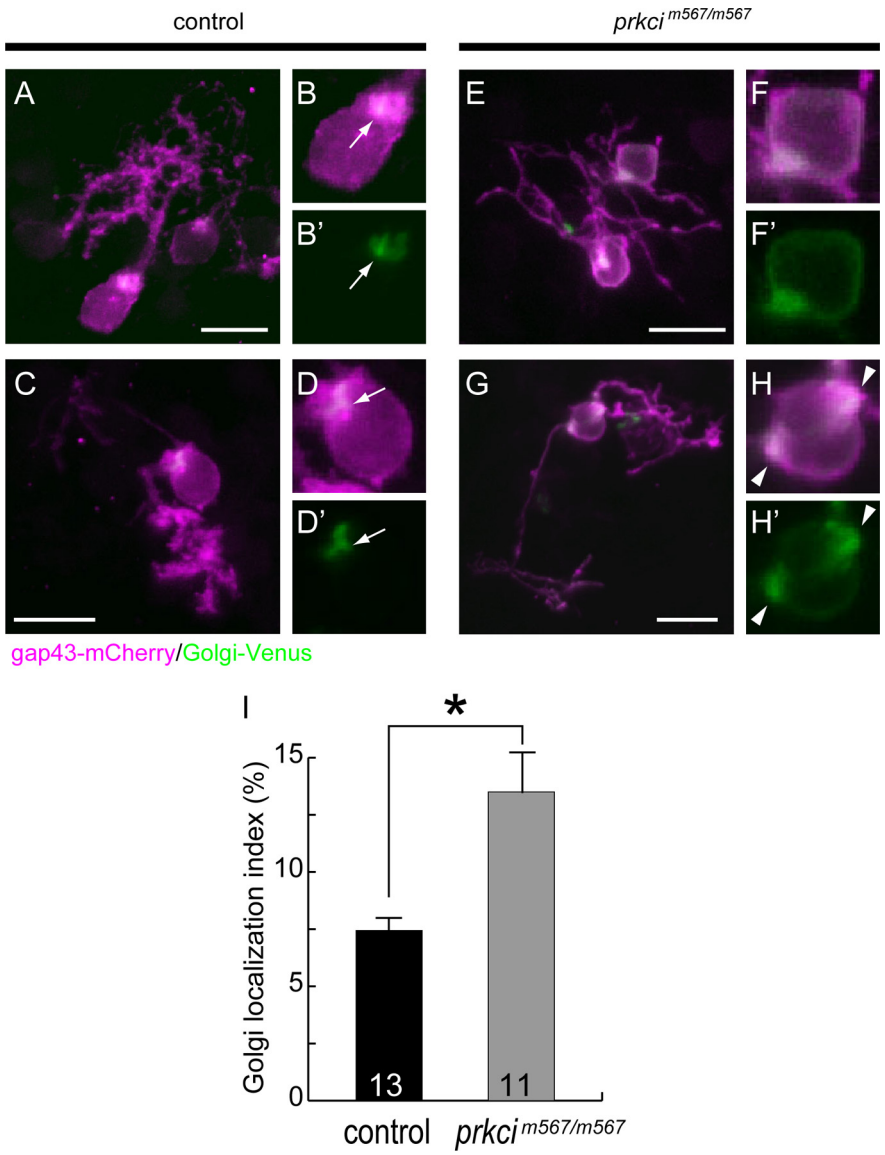

Figure 6. Golgi localization is disrupted in *prkci* mutant larvae. ***A–H′***, Purkinje cells from *aldoca:gap43-mCherry-PTV1-2A-Golgi-Venus*-injected 4.5 dpf control (***A–D′***) and *prkci* mutant (***E–H′***) larvae. ***A***, ***C***, ***E***, ***G***, Anteromedial Purkinje cells (***A***, ***E***) and posterolateral Purkinje cells (***C***, ***G***). All images are dorsal view projected images. ***B***, ***B′***, ***D***, ***D′***, ***F***, ***F′***, ***H***, ***H′***, High-magnification views near the soma. In the control Purkinje cells, Golgi-Venus was exclusively localized to the root of a single primary dendrite (***B***, ***B′***, ***D***, ***D′***, arrows). In contrast, Golgi-Venus was more uniformly distributed in the *prkci* mutant Purkinje cells, although a strong accumulation was still detected. In one particular case, multiple spots of strong Golgi-Venus accumulation were observed, and two primary dendrites extended from sites adjacent to these accumulations (***H***, ***H′***, arrowheads). ***I***, Graph of the Golgi localization index of control (black bar) and *prkci* mutant (gray bar) Purkinje cells. The Golgi localization index was calculated as the percentage of the area of Golgi apparatus over the somal area (see Materials and Methods). The Golgi localization index was significantly increased in the Purkinje cells of *prkci* mutant larvae (*$p < 0.01$ by Welch's *t* test). Error bars show SEM. Numbers inside the bars represent the number of cells tested. Scale bars, 10 μm.

function of Prkci recapitulated the multidendrite phenotype and the aberrant Golgi localization in the *prkci* mutants, suggesting that Prkci cell autonomously controls the Golgi localization and subsequent specification of a single primary dendrite in postmitotic Purkinje cells.

Although *prkci* mutant and *prkci*^{2A}-expressing Purkinje cells showed multidendrite phenotype and aberrant Golgi localization, they showed different dendritic morphology. Purkinje cells in the *prkci* mutants had simpler dendrites and did not have dendritic spines (Fig. 5*B*,*E*), whereas *prkci*^{2A}-expressing Purkinje cells developed highly branched dendritic arbors and dense spines (Fig. 7*E*,*G*). We measured the dendritic area of Purkinje cells in the *prkci* mutants at 4.5 dpf and *prkci*^{2A}-expressing Purkinje cells at 5.5 dpf. The dendritic area of Purkinje cells in control larvae was 144.8 μm^2 on average ($n = 11$, SEM = 16.03 μm^2), whereas the Purkinje cells in *prkci* mutant larvae had smaller dendritic area (81.82 μm^2 on average, $n = 11$, SEM = 20.20 μm^2, $p < 0.05$) (supplemental Fig. 2*A*, available at www.jneurosci.org as supplemental material) at 4.5 dpf. In contrast, we did not detect significant changes in the dendritic area of the *prkci*^{2A}-expressing Purkinje cells (174.6 μm^2 on average, $n = 12$, SEM = 13.11 μm^2), compared with that of control Purkinje cells at 5.5 dpf (180.8 μm^2 on average, $n = 10$, SEM = 15.60 μm^2, $p > 0.5$) (supplemental Fig. 2*B*, available at www.jneurosci.org as supplemental material). Furthermore, expression of *prkci*^{2A} did not perturb the formation of Purkinje cells axons that project to either a eurydendroid cell or a neighboring Purkinje cell (data not shown). Collecting together, our findings indicate that, although Prkci may indirectly control the growth and maturation of Purkinje cell dendrites, the Prkci cell autonomously regulates the Golgi localization and the subsequent primary dendrite specification in Purkinje cells.

Discussion

Dendritic morphology of Purkinje cells in the zebrafish cerebellum

In this study, we observed that, unlike Purkinje cells in the mammalian cerebellum, which all display a similar dendritic morphology, zebrafish Purkinje cells displayed morphological diversity that varied according to the somal location. Purkinje cells in the posterolateral domain exhibited a relatively planar pattern of dendrites, which is a characteristic of mammalian Purkinje cells. In contrast, Purkinje cells in the anteromedial domain extended the single primary dendrite that branched extensively and did not show a planar pattern (Fig. 1). Since the latest stage at which we performed the imaging was 8 dpf, it is possible that the morphological diversity was transient. In the corpus cerebelli of the adult zebrafish cerebellum, which includes the regions corresponding to both the anteromedial and posterolateral domains at the larval stage, Purkinje cells do not show an obvious planar dendritic morphology (Bae et al., 2009), but the dendrites of Purkinje cells in the adult valvula cerebelli, the rostral part of the cerebellum, seem to be packed into a planar structure (Miyamura and Nakayasu, 2001). Furthermore, Purkinje cell dendrites of the mormyrid fish show a highly polarized structure in the valvula cerebelli (Meek et al., 2008; Shi et al., 2008). Thus, further single-cell labeling studies are needed to reveal the precise structures of Purkinje cell dendrites at later developmental stages.

It is worth noting that, in the early larva, the parallel fibers run perpendicular to the anteroposterior axis in the posterior domain of the cerebellum (Volkmann et al., 2008; Bae et al., 2009). This is where the Purkinje cells extend a primary dendrite and develop dendritic spines that have a postsynaptic marker (8 dpf, data not shown) and possibly contact the parallel fibers. Therefore, the planar polarity seen in the posterior Purkinje cell dendrites is likely to play a role in the formation of neural circuits during the larval period. Future analysis of the functional characterizations of individual Purkinje cells (e.g., differences in their axonal projection patterns) should shed additional light on the importance of this morphological diversity.

Specification of a single primary dendrite in Purkinje cells

In the rodent cerebellum, Purkinje cells dramatically change their morphology during postnatal development (Armengol and Sotelo, 1991; Kapfhammer, 2004). In the first postnatal week, Purkinje cells extend multiple dendrites and exhibit a "disoriented" morphology. During the second postnatal week, Purkinje cells become morphologically polarized by retracting all the transient dendrites except for a single, permanent primary dendrite, which branches extensively and forms numerous synapses. Here, we found that in zebrafish immature Purkinje cells also extended multiple dendrites at ~3 dpf (Fig. 2). The Purkinje cells showed dynamic morphological remodeling of the neurites and retracted all but one, which became the primary dendrite (Fig. 2). Therefore, the dendritic morphogenesis of cerebellar Purkinje cells is conserved between zebrafish and mammals.

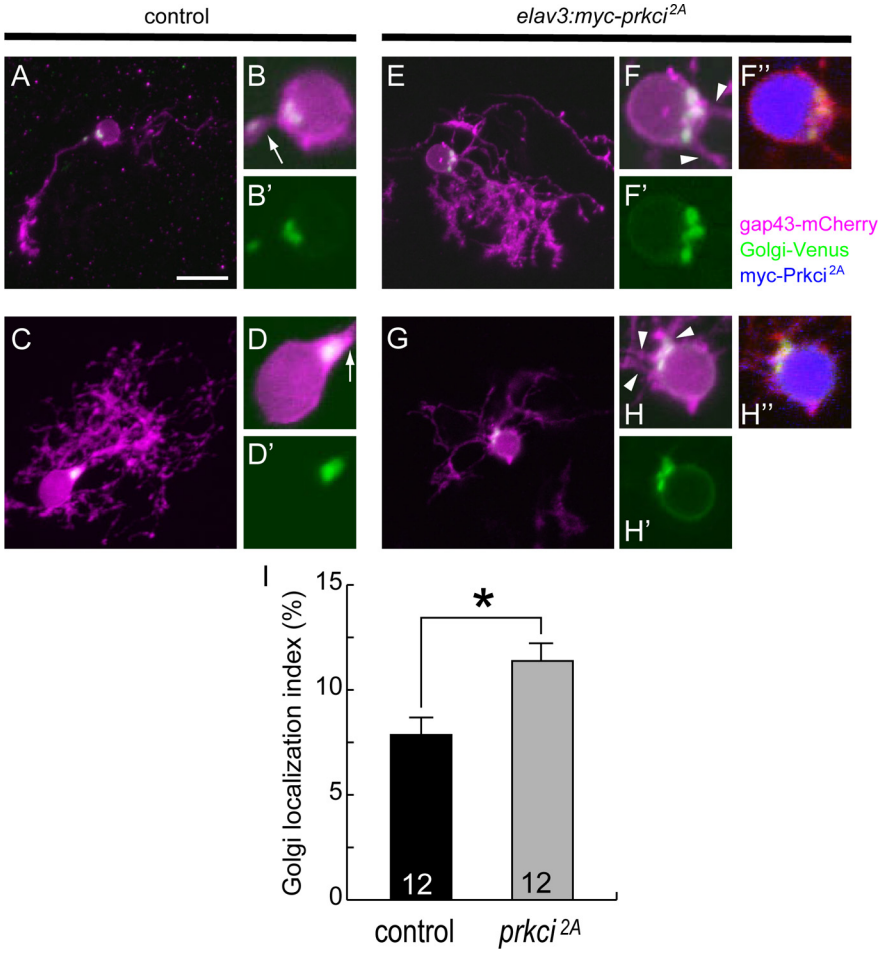

Figure 7. Prkci is required cell autonomously for establishing the proper Golgi localization and selection of the primary dendrite. ***A–H″***, Purkinje cells from 5 dpf larvae expressing *aldoca:gap43-mCherry-PTV1–2A-Golgi-Venus* alone (***A–D′***, control) or with *elavl3:myc-prkci*^{2A} (***E–H″***). All are dorsal view projected images. ***B***, ***B′***, ***D***, ***D′***, ***F***, ***F′***, ***F″***, ***H***, ***H′***, ***H″***, High-magnification views near the soma. Control Purkinje cells extended a single primary dendrite, and Golgi-Venus (green) was exclusively localized to the root of a single primary dendrite (arrows). Purkinje cells that expressed myc-Prkci ^{2A} (blue) extended multiple primary dendrites, and the Golgi-Venus $^{+}$ region was expanded. Extra primary dendrites were extended from adjacent sites to the expanded Golgi (arrowheads). ***I***, Graph of the Golgi localization index of control Purkinje cells (black bar) and Purkinje cells expressing myc-Prkci ^{2A} (gray bar). The Golgi localization index was significantly increased in the Purkinje cells expressing myc-Prkci ^{2A} (*$p < 0.01$ in Welch's *t* test). Error bars show SEM. Numbers inside the bars represent the number of cells tested. All cells are shown in the same scale. Scale bars, 10 μm.

Role for the Golgi apparatus in the primary dendrite specification of Purkinje cells

As a possible mechanism for the primary dendrite specification of Purkinje cells, we focused on the localization of the Golgi apparatus, which we found was located adjacent to the primary dendrite of mature Purkinje cells (Fig. 3). Importantly, the Golgi localization preceded the primary dendrite specification, suggesting that the localized Golgi apparatus plays an instructive role in the selection of the primary dendrite. The BFA treatment experiment (Fig. 4) showed that secretory trafficking through the Golgi promotes dendritic growth, as previously reported for rodent hippocampal and cortical pyramidal cells, and *Drosophila* dendritic arborization neurons (Horton et al., 2005; Ye et al., 2007). We found that the BFA treatment did not perturb the primary dendrite specification (Fig. 4). This is likely due to incomplete inhibition of the Golgi-mediated secretory trafficking by the BFA treatment, and the remaining trafficking activity may be sufficient for the primary dendrite specification. The data clearly indicate that localized Golgi-mediated trafficking is required for the dendritic growth of Purkinje cells (Fig. 4). Together with these previous reports, our observations suggest that the localization of the Golgi apparatus could be a common mechanism by which neurons generate their asymmetric dendritic morphology.

Compared with the Golgi apparatus of pyramidal cells in the rodent hippocampus and cortex, which have multiple dendrites as well as an asymmetric dendritic morphology (Horton et al., 2005), the Golgi apparatus in Purkinje cells is restricted to a more limited domain, reflecting the highly polarized dendritic morphology. It will be interesting to learn whether the Golgi apparatus is strictly located at the root of the primary dendrite of other neurons that have a single primary dendrite, such as retinal bipolar cells. Golgi outposts, which are Golgi apparatuses located in dendritic arbors distant from the soma, play a critical role in dendritic branching (Horton et al., 2005; Ye et al., 2007). Although the zebrafish Purkinje cell dendrites branch extensively, we did not find any Golgi apparatuses in their dendritic trees. Thus, the Golgi apparatus plays two distinct roles in dendrite formation: as Golgi outposts, its function is to provide complex dendritic morphologies; located at the root of a neurite, its role is to determine the primary dendrite.

Role for aPKC in the primary dendrite specification of Purkinje cells

We also found that aPKC *prkci* is necessary for the proper distribution of the Golgi apparatus and the subsequent primary dendrite specification. The Par3/Par6/aPKC complex is reported to be a fundamental determinant for axon specification in cultured neurons (Shi et al., 2003), although some reports claim that these molecules are not involved in axon specification *in vivo*. Neither their genetic mutations nor the overexpression of each of these apical complex components affects axon and dendrite morphology in *Drosophila* mushroom body neurons (Rolls and Doe, 2004). In the zebrafish retina, retinal ganglion cells form axons independent of Par-3 localization, and they efficiently polarize and extend axons in the *prkci*-deficient mutant (Zolessi et al., 2006). Although the cerebellovestibular axons of Purkinje cells were affected in the *prkci* mutant larvae, the *prkci*^{2A}-expressing Purkinje cells normally extended an axon to a eurydendroid cell or a neighboring Purkinje cell (data not shown), suggesting the major role of Prkci in Purkinje cells in the primary dendrite specification. The discrepancy in the function of the Par complex between these studies and ours could be due to the difference between *in vivo* and *in vitro* conditions. Alternatively, the complex might function differently in the polarization of different kinds of neurons.

aPKC and Par6 influence the localization of the Golgi apparatus in migrating astrocytes (Etienne-Manneville and Hall, 2001) and rat primary fibroblasts (Cau and Hall, 2005), in which the Golgi polarization is essential for their directed migration. Our results indicate that the aPKC Prkci affects the Golgi localization in Purkinje cells. Therefore, aPKC has a common function in controlling the Golgi localization in various cell types and different biological phenomena.

Where Prkci is located during the primary dendrite specification of Purkinje cells and how its location is regulated remain to be discovered. Although we immunostained zebrafish larvae with an antibody that recognizes Prkci (data not shown), we did not observe its specific subcellular localization in Purkinje cells. Even if there was some preferential localization, the noise from the Prkci labeling, seen in all cerebellar neurons, might make pinpointing the subcellular localization of Prkci quite difficult. More specific and sensitive methods for detecting the localization of Prkci are needed. We also tried expressing Pard3-EGFP (ASIP-EGFP) and EGFP-Pard6α in Purkinje cells. Although the fusion proteins are known to be located at the apical surface of the neuroepithelium, recapitulating their endogenous localization (Geldmacher-Voss et al., 2003; Munson et al., 2008), they showed relative uniform distribution along the plasma membrane of Purkinje cells (data not shown). There are a few possible explanations for this lack of specific expression. First, it is possible that only active form(s) of aPKC, Par3, or Par6 (or the entire complex) are located in the soma of Purkinje cells, and the active form controls the Golgi localization. Second, a small difference in the levels of these components might amplify a signal that controls Golgi localization. Alternatively, aPKC or the Par complex by itself may not directly control Golgi localization; instead it might cooperate with another signal that determines Golgi localization and/or controls the primary dendrite specification. Future identification of active aPKC localization and of the signals that act upstream, downstream, or in parallel to aPKC should clarify this issue.

Other possible mechanisms controlling the primary dendrite specification of Purkinje cells

Extracellular factors could also regulate the primary dendrite specification of Purkinje cells. There are many reports suggesting that other cells in the cerebellum, especially granule cells, affect the dendritic morphogenesis of Purkinje cells. When the number of granule cells is reduced by x-ray irradiation or a genetic mutation in the rodent cerebellum, the dendritic morphogenesis of the Purkinje cells is disorganized (Altman and Anderson, 1972; Rakic and Sidman, 1973). Furthermore, in a dissociated culture of cerebellar neurons, the cell–cell interaction between Purkinje and granule cells is critical for Purkinje cell dendritic growth and spine formation (Baptista et al., 1994). A neurotrophic factor and electrical activity are suggested factors that could be presented by parallel fibers and regulate the dendritic morphogenesis of Purkinje cells (Schwartz et al., 1997; Hirai and Launey, 2000). We found that the Purkinje cells of *prkci* mutants showed more severe defects in Golgi localization and primary dendrite formation than those expressing the dominant-negative Prkci (Figs. 6, 7). Furthermore, Purkinje cells showed smaller dendritic area in the *prkci* mutant larvae than control larvae, whereas the *prkci*^{2A}-expressing Purkinje cells had comparable dendritic area to control Purkinje cells (supplemental Fig. 2, available at www.jneurosci.org as supplemental material). The *prkci* mutants showed a strong reduction or absence of parallel fibers (data not shown), which might affect the morphogenesis of Purkinje cell dendrites.

Inputs from climbing fibers are also thought to play a role in Purkinje cell dendrogenesis. It is, however, unlikely that climbing fibers influence the primary dendrite specification of Purkinje cells in zebrafish, because they are not detected until after 4 dpf, when the polarization takes place (Punnamoottil et al., 2008; Bae et al., 2009). We previously isolated mutants with defects in the neurite formation of Purkinje and/or granule cells (Bae et al., 2009). Further analyses, including studies of these mutants, should provide insight into the intrinsic and extracellular cues that regulate Golgi localization and the primary dendrite specification of Purkinje cells.

References

Altman J, Anderson WJ (1972) Experimental reorganization of the cerebellar cortex. I. Morphological effects of elimination of all microneurons with prolonged x-irradiation started at birth. J Comp Neurol 146:355–406.

Arimura N, Kaibuchi K (2007) Neuronal polarity: from extracellular signals to intracellular mechanisms. Nat Rev Neurosci 8:194–205.

Armengol JA, Sotelo C (1991) Early dendritic development of Purkinje cells in the rat cerebellum. A light and electron microscopic study using axonal tracing in "in vitro" slices. Brain Res Dev Brain Res 64:95–114.

Bae YK, Kani S, Shimizu T, Tanabe K, Nojima H, Kimura Y, Higashijima S, Hibi M (2009) Anatomy of zebrafish cerebellum and screen for mutations affecting its development. Dev Biol 330:406–426.

Baptista CA, Hatten ME, Blazeski R, Mason CA (1994) Cell-cell interactions influence survival and differentiation of purified Purkinje cells in vitro. Neuron 12:243–260.

Brochu G, Maler L, Hawkes R (1990) Zebrin II: a polypeptide antigen expressed selectively by Purkinje cells reveals compartments in rat and fish cerebellum. J Comp Neurol 291:538–552.

Cau J, Hall A (2005) Cdc42 controls the polarity of the actin and microtubule cytoskeletons through two distinct signal transduction pathways. J Cell Sci 118:2579–2587.

Dotti CG, Sullivan CA, Banker GA (1988) The establishment of polarity by hippocampal neurons in culture. J Neurosci 8:1454–1468.

Etienne-Manneville S, Hall A (2001) Integrin-mediated activation of Cdc42 controls cell polarity in migrating astrocytes through PKCzeta. Cell 106:489–498.

Geldmacher-Voss B, Reugels AM, Pauls S, Campos-Ortega JA (2003) A 90-degree rotation of the mitotic spindle changes the orientation of mitoses of zebrafish neuroepithelial cells. Development 130:3767–3780.

Higashijima S, Okamoto H, Ueno N, Hotta Y, Eguchi G (1997) High-frequency generation of transgenic zebrafish which reliably express GFP in whole muscles or the whole body by using promoters of zebrafish origin. Dev Biol 192:289–299.

Higashijima S, Masino MA, Mandel G, Fetcho JR (2003) Imaging neuronal activity during zebrafish behavior with a genetically encoded calcium indicator. J Neurophysiol 90:3986–3997.

Hirai H, Launey T (2000) The regulatory connection between the activity of granule cell NMDA receptors and dendritic differentiation of cerebellar Purkinje cells. J Neurosci 20:5217–5224.

Horne-Badovinac S, Lin D, Waldron S, Schwarz M, Mbamalu G, Pawson T, Jan Y, Stainier DY, Abdelilah-Seyfried S (2001) Positional cloning of heart and soul reveals multiple roles for PKC lambda in zebrafish organogenesis. Curr Biol 11:1492–1502.

Horton AC, Rácz B, Monson EE, Lin AL, Weinberg RJ, Ehlers MD (2005) Polarized secretory trafficking directs cargo for asymmetric dendrite growth and morphogenesis. Neuron 48:757–771.

Hoshino M, Nakamura S, Mori K, Kawauchi T, Terao M, Nishimura YV, Fukuda A, Fuse T, Matsuo N, Sone M, Watanabe M, Bito H, Terashima T, Wright CV, Kawaguchi Y, Nakao K, Nabeshima Y (2005) Ptf1a, a bHLH transcriptional gene, defines GABAergic neuronal fates in cerebellum. Neuron 47:201–213.

Jan YN, Jan LY (2010) Branching out: mechanisms of dendritic arborization. Nat Rev Neurosci 11:316–328.

Jensen AM, Westerfield M (2004) Zebrafish mosaic eyes is a novel FERM protein required for retinal lamination and retinal pigmented epithelial tight junction formation. Curr Biol 14:711–717.

Kani S, Bae YK, Shimizu T, Tanabe K, Satou C, Parsons MJ, Scott E, Higashijima S, Hibi M (2010) Proneural gene-linked neurogenesis in zebrafish cerebellum. Dev Biol 343:1–17.

Kapfhammer JP (2004) Cellular and molecular control of dendritic growth and development of cerebellar Purkinje cells. Prog Histochem Cytochem 39:131–182.

Kawakami K, Takeda H, Kawakami N, Kobayashi M, Matsuda N, Mishina M (2004) A transposon-mediated gene trap approach identifies developmentally regulated genes in zebrafish. Dev Cell 7:133–144.

Kay JN, Roeser T, Mumm JS, Godinho L, Mrejeru A, Wong RO, Baier H (2004) Transient requirement for ganglion cells during assembly of retinal synaptic layers. Development 131:1331–1342.

Kimmel CB, Ballard WW, Kimmel SR, Ullmann B, Schilling TF (1995) Stages of embryonic development of the zebrafish. Dev Dyn 203:253–310.

Klausner RD, Donaldson JG, Lippincott-Schwartz J (1992) Brefeldin A: insights into the control of membrane traffic and organelle structure. J Cell Biol 116:1071–1080.

Lannoo MJ, Ross L, Maler L, Hawkes R (1991a) Development of the cerebellum and its extracerebellar Purkinje cell projection in teleost fishes as determined by zebrin II immunocytochemistry. Prog Neurobiol 37:329–363.

Lannoo MJ, Brochu G, Maler L, Hawkes R (1991b) Zebrin II immunoreactivity in the rat and in the weakly electric teleost Eigenmannia (gymnotiformes) reveals three modes of Purkinje cell development. J Comp Neurol 310:215–233.

Llopis J, McCaffery JM, Miyawaki A, Farquhar MG, Tsien RY (1998) Measurement of cytosolic, mitochondrial, and Golgi pH in single living cells with green fluorescent proteins. Proc Natl Acad Sci U S A 95:6803–6808.

Marzban H, Chung SH, Pezhouh MK, Feirabend H, Watanabe M, Voogd J, Hawkes R (2010) Antigenic compartmentation of the cerebellar cortex in the chicken (Gallus domesticus). J Comp Neurol 518:2221–2239.

Meek J, Hafmans TG, Maler L, Hawkes R (1992) Distribution of zebrin II in the gigantocerebellum of the mormyrid fish Gnathonemus petersii compared with other teleosts. J Comp Neurol 316:17–31.

Meek J, Yang JY, Han VZ, Bell CC (2008) Morphological analysis of the mormyrid cerebellum using immunohistochemistry, with emphasis on the unusual neuronal organization of the valvula. J Comp Neurol 510:396–421.

Miyamura Y, Nakayasu H (2001) Zonal distribution of Purkinje cells in the zebrafish cerebellum: analysis by means of a specific monoclonal antibody. Cell Tissue Res 305:299–305.

Munson C, Huisken J, Bit-Avragim N, Kuo T, Dong PD, Ober EA, Verkade H, Abdelilah-Seyfried S, Stainier DY (2008) Regulation of neurocoel morphogenesis by Pard6 gamma b. Dev Biol 324:41–54.

Nagai T, Ibata K, Park ES, Kubota M, Mikoshiba K, Miyawaki A (2002) A variant of yellow fluorescent protein with fast and efficient maturation for cell-biological applications. Nat Biotechnol 20:87–90.

Okada A, Lansford R, Weimann JM, Fraser SE, McConnell SK (1999) Imaging cells in the developing nervous system with retrovirus expressing modified green fluorescent protein. Exp Neurol 156:394–406.

Omori Y, Malicki J (2006) oko meduzy and related crumbs genes are determinants of apical cell features in the vertebrate embryo. Curr Biol 16:945–957.

Ozol K, Hayden JM, Oberdick J, Hawkes R (1999) Transverse zones in the vermis of the mouse cerebellum. J Comp Neurol 412:95–111.

Park HC, Kim CH, Bae YK, Yeo SY, Kim SH, Hong SK, Shin J, Yoo KW, Hibi M, Hirano T, Miki N, Chitnis AB, Huh TL (2000) Analysis of upstream elements in the HuC promoter leads to the establishment of transgenic zebrafish with fluorescent neurons. Dev Biol 227:279–293.

Parrish JZ, Emoto K, Kim MD, Jan YN (2007) Mechanisms that regulate establishment, maintenance, and remodeling of dendritic fields. Annu Rev Neurosci 30:399–423.

Provost E, Rhee J, Leach SD (2007) Viral 2A peptides allow expression of multiple proteins from a single ORF in transgenic zebrafish embryos. Genesis 45:625–629.

Punnamoottil B, Kikuta H, Pezeron G, Erceg J, Becker TS, Rinkwitz S (2008) Enhancer detection in zebrafish permits the identification of neuronal subtypes that express Hox4 paralogs. Dev Dyn 237:2195–2208.

Rakic P, Sidman RL (1973) Organization of cerebellar cortex secondary to deficit of granule cells in weaver mutant mice. J Comp Neurol 152:133–161.

Rohr S, Bit-Avragim N, Abdelilah-Seyfried S (2006) Heart and soul/PRKCi and nagie oko/Mpp5 regulate myocardial coherence and remodeling during cardiac morphogenesis. Development 133:107–115.

Rolls MM, Doe CQ (2004) Baz, Par-6 and aPKC are not required for axon or dendrite specification in Drosophila. Nat Neurosci 7:1293–1295.

Sato T, Takahoko M, Okamoto H (2006) HuC:Kaede, a useful tool to label neural morphologies in networks in vivo. Genesis 44:136–142.

Schwartz PM, Borghesani PR, Levy RL, Pomeroy SL, Segal RA (1997) Abnormal cerebellar development and foliation in BDNF-/- mice reveals a role for neurotrophins in CNS patterning. Neuron 19:269–281.

Shaner NC, Campbell RE, Steinbach PA, Giepmans BN, Palmer AE, Tsien RY (2004) Improved monomeric red, orange and yellow fluorescent proteins derived from Discosoma sp. red fluorescent protein. Nat Biotechnol 22:1567–1572.

Shi SH, Jan LY, Jan YN (2003) Hippocampal neuronal polarity specified by spatially localized mPar3/mPar6 and PI 3-kinase activity. Cell 112:63–75.

Shi Z, Zhang Y, Meek J, Qiao J, Han VZ (2008) The neuronal organization of a unique cerebellar specialization: the valvula cerebelli of a mormyrid fish. J Comp Neurol 509:449–473.

Stuart GW, McMurray JV, Westerfield M (1988) Replication, integration and stable germ-line transmission of foreign sequences injected into early zebrafish embryos. Development 103:403–412.

Suzuki A, Ohno S (2006) The PAR-aPKC system: lessons in polarity. J Cell Sci 119:979–987.

Tanaka M, Yanagawa Y, Obata K, Marunouchi T (2006) Dendritic morphogenesis of cerebellar Purkinje cells through extension and retraction revealed by long-term tracking of living cells in vitro. Neuroscience 141:663–674.

Volkmann K, Rieger S, Babaryka A, Köster RW (2008) The zebrafish cerebellar rhombic lip is spatially patterned in producing granule cell populations of different functional compartments. Dev Biol 313:167–180.

Wei X, Malicki J (2002) nagie oko, encoding a MAGUK-family protein, is essential for cellular patterning of the retina. Nat Genet 31:150–157.

Westerfield M (1993) The zebrafish book: a guide for the laboratory use of zebrafish (Brachydanio rerio). Eugene, OR: M. Westerfield.

Ye B, Zhang Y, Song W, Younger SH, Jan LY, Jan YN (2007) Growing dendrites and axons differ in their reliance on the secretory pathway. Cell 130:717–729.

Zolessi FR, Poggi L, Wilkinson CJ, Chien CB, Harris WA (2006) Polarization and orientation of retinal ganglion cells in vivo. Neural Dev 1:2.